

Article

Study on the Influence of Particle Size Distribution on the Separation of Pyrite from Coal Gangue by Jigging

Xinkai Hou ^{1,*}, Zhentong Xi ^{1,†}, Xiangfeng Wang ^{1,2} and Wenjuan Ji ¹

¹ College of Materials Science and Engineering, Xi'an University of Architecture and Technology, Xi'an 710055, China; 15596707931@163.com (Z.X.); wxf07272024@126.com (X.W.); 19916415835@163.com (W.J.)

² Ansteel Iron and Steel Research Institute, Anshan 114009, China

* Correspondence: houxinkai1@xauat.edu.cn

† These authors contributed equally to this work.

Abstract: The presence of pyrite poses a significant impediment to the comprehensive utilization of coal gangue, which is a prevalent solid waste in industrial production. However, the current efficacy of jig separation for pyrite in fine-grade coal gangue remains unsatisfactory. To investigate the influence of particle size distribution on the jig separation of pyrite in fine-grade coal gangue, the raw material was crushed to less than 2 mm using a jaw crusher and subsequently sieved to obtain its particle size distribution curve. Upon fitting the curve, it was observed that it tends towards the Rosin-Rammler (RRSB) and Fuller distributions. Leveraging these two-parameter distribution curves, adjustments were made to determine the mass within each particle size range before conducting thorough mixing followed by jig separation. The results indicate that for fine-grade gangue particles smaller than 2 mm, the RRSB distribution with a uniformity coefficient of $n = 0.85$ exhibits the most effective separation, although it is comparable to the separation achieved using the size distribution of raw ore. On the other hand, employing the Fuller distribution with modulus of distribution $q = 1.5$ yields superior separation performance. In comparison to the raw ore, the concentrate shows an increase in sulfur (S) and iron (Fe) content by factors of 3.4 and 2.4, respectively. Furthermore, compared to the RRSB distribution, there is an increase in S and Fe content by 1.91% and 2.30%, respectively; the contents of S and Fe in tailings is 0.71% and 2.72%, which can be directly used as raw materials for coating materials. Therefore, for fine-grade coal gangue particles, jigging under the Fuller distribution demonstrates better effectiveness than under the RRSB distribution.



Citation: Hou, X.; Xi, Z.; Wang, X.; Ji, W. Study on the Influence of Particle Size Distribution on the Separation of Pyrite from Coal Gangue by Jigging. *Coatings* **2024**, *14*, 610. <https://doi.org/10.3390/coatings14050610>

Academic Editor: Paolo Castaldo

Received: 14 April 2024

Revised: 7 May 2024

Accepted: 9 May 2024

Published: 11 May 2024



Copyright: © 2024 by the authors. Licensee MDPI, Basel, Switzerland. This article is an open access article distributed under the terms and conditions of the Creative Commons Attribution (CC BY) license (<https://creativecommons.org/licenses/by/4.0/>).

Keywords: coal gangue; jig separation; pyrite; particle size distribution; Rosin-Ramler distribution; Fuller distribution; coating materials

1. Introduction

Coal gangue is a solid waste generated during coal mining [1], characterized by its low carbon content, which leads to a range of environmental issues due to its limited utilization and extensive accumulation [2–4]. Moreover, the presence of pyrite in coal gangue increases the risk of spontaneous combustion as sulfur easily oxidizes, further hindering comprehensive utilization [5,6]. On one hand, high-sulfur pyrite can be utilized for economic benefits through sulfuric acid production [7]. On the other hand, tailings devoid or containing minimal amounts of pyrite can be employed in building material manufacturing [8]. Therefore, the separation of pyrite in coal gangue is different from the ordinary descaling process. The ordinary descaling process is to separate impurities and make use of valuable concentrate or tailings. The pyrite concentrate and tailings produced by coal gangue separation have their utilization value, and the separation products can be fully utilized as resources, which is also an important reason for the comprehensive utilization rate of coal gangue to be improved [9].

The separation of pyrite from coal gangue is mainly carried out by gravity separation [10], and less by flotation and electric separation. The gravity separation equipment

mainly includes a jig, shaker and cyclone. Jigging has the advantages of wide separation particle size range, a large processing capacity and simple process [11], and is an ideal method for the separation of coal gangue and coal measure minerals. Phengsaart, T. [12] developed a microencapsulated hybrid jig separation technology that combines the flotation delamination concept based on the apparent specific gravity of the particles. At the same time, the microencapsulated technology (a method of encapsulating the target material with a protective coating) overcomes the disadvantages of the low separation efficiency of traditional methods. The separation efficiency of pyrite and coal in the range of 1–4 mm particle size is improved. Viduka, S. [13] modeled the liquid–solid system during jig separation by simulating the analytical motion of a liquid flow discrete element (DEM) through combined computational dynamics (CFM). Changing the amplitude and frequency of the jig, and comparing the energy, power and relative position of coal gangue particles to determine the best parameters, improves the separation effect. But at present, the research of coal gangue jig separation is mostly about the technological parameters [14,15] and mechanical structure [16]. There is little research on the properties of materials, and the jig has a poor effect on the separation of connected minerals with fine particle size [17]. Therefore, the influence of fine particle size materials with different particle size distribution on the jig separation is investigated in this paper.

In recent years, particle size analysis [18,19] has been widely used in the study of fine dust materials. The normal distribution [20], lognormal distribution [21], Fuller distribution [22] and Rosin-Rammler (RRSB) distribution [23]. These are the functional models commonly used to express the grain size distribution of fine powder materials. Yunpeng Cui [24] used fly ash as the admixture of concrete, and selected fly ash with different particle size distributions to prepare concrete. The relationship between the particle size distribution of fly ash, compressive strength, hydration, pore structure and the microstructure of concrete is studied. Peng Gao [25] described the particle size distribution of graded mixed cement components (PSD) based on the Rosin-Rammler (RRSB) distribution and lognormal distribution. It is found that the lognormal distribution exhibits a small fitting error when described. More importantly, the lognormal distribution exhibits good simplicity and popularity. Weichen Sun [26] proposes an algorithm based on particle population probability distribution (PNPD), which is verified by two classical gradient curves of the Rosin-Rammler curve and the Fuller curve. Not only is the grade of granular samples in the whole sample verified, but also the local location of the generated samples. In addition, the PNPD algorithm can dynamically generate graded granular materials on the conveyor belt in two and three dimensions, which is consistent with the actual situation.

The study of the particle size distribution of fine powder has been applied in many aspects [27,28], but there are still few studies on jigging separation by particle size distribution. In view of this, taking coal gangue as the research object, the raw ore is crushed to –2 mm by a jaw crusher and sieved, and the cumulative distribution curve is drawn with the particle size as the horizontal coordinate, and the determination coefficient R^2 [29–31] is used as the determination index to determine the distribution curve of the raw ore. According to the particle size distribution that the raw ore tends to meet, the parameters are changed to make the mass proportion of the material in each particle size range different, and the jig separation is carried out after the material is evenly mixed. This study revealed the separation effect under different parameter distributions, verified the influence of particle size distribution on jig separation, and provided a new beneficiation scheme for coal gangue separation.

2. Materials and Methods

2.1. Materials

The experimental coal gangue is sourced from Ningwu, Shanxi, and its primary chemical components [32] include Al_2O_3 , SiO_2 , Fe_2O_3 , SO_3 , CaO , MgO , Na_2O , K_2O , P_2O_5 , as shown in Table 1. The sample contains 2.19% sulfur (S), mainly in the form of pyrite.

The total iron content (TFe) is 5.36%, indicating that it belongs to medium-sulfur coal gangue [33].

Table 1. Chemical composition of coal gangue.

Sample	SiO ₂	Al ₂ O ₃	Fe ₂ O ₃	SO ₃	CaO	K ₂ O	TiO ₂	MgO	ZrO ₂	P ₂ O ₅	Na ₂ O	Total
Content (%)	55.61	24.15	7.55	5.48	2.63	2.37	1.13	0.32	0.15	0.11	0.09	99.59

The main minerals [34,35] present in coal gangue include quartz, kaolinite, dolomite, and pyrite, along with a small amount of calcite as depicted in Figure 1. Table 2 displays the densities of these primary minerals. It is evident from the table that there exists significant disparity in density between pyrite and other minerals within coal gangue. Jig separation involves stratifying coal gangue particles based on their density and particle size to achieve effective separation [36]. Hence, employing a jig for separating pyrite from coal gangue is indeed feasible.

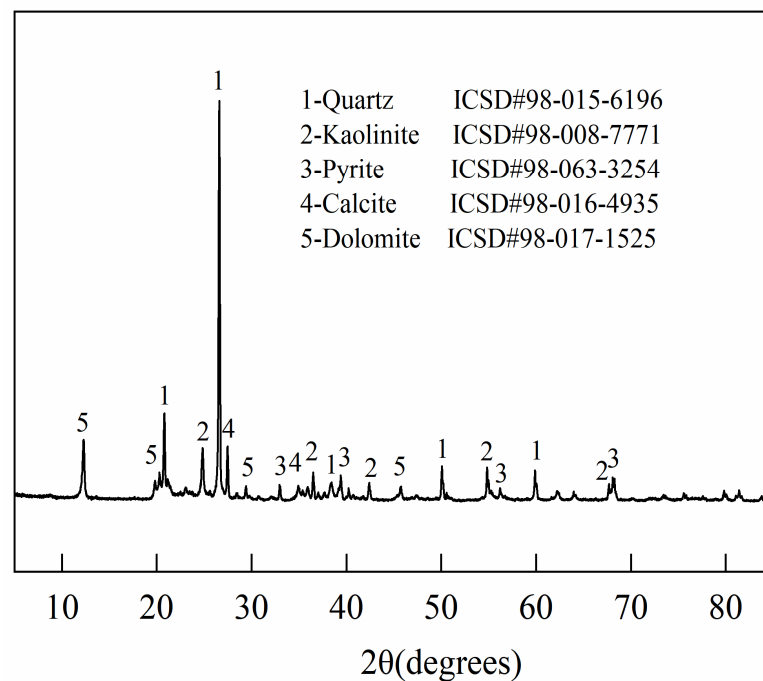


Figure 1. XRD pattern of coal gangue sample.

Table 2. Main mineral density of coal gangue.

Sample	Pyrite (FeS ₂)	Calcite (CaCO ₃)	Dolomite CaMg(CO ₃) ₂	Quartz (SiO ₂)	Kaolinite (Al ₂ H ₄ O ₉ Si ₂)
Density (g/cm ³)	4.9~5.2	2.71	2.8~2.9	2.65	2.60~2.63

2.2. Particle Size Distribution

The raw coal gangue was crushed to a size of -2 mm using a jaw crusher and then sieved with a vibration sieve. A particle size distribution diagram was plotted, with the horizontal axis representing particle size and the vertical axis representing cumulative distribution, and the distribution type is shown in Figure 2.

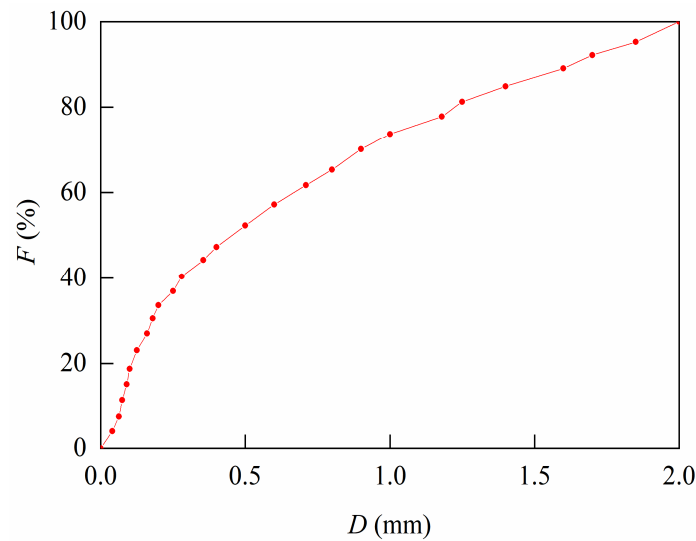


Figure 2. Grain size distribution curve.

2.3. Samples Proportioning Scheme

2.3.1. Samples under RRSB Distribution

The distribution of RRSB involves the examination of the probability and statistical theory of fine particle size materials. The relationship of particle size distribution is expressed by the following exponential function:

$$F(D) = 100 - R = 100 - 100 \exp[-(D/D_e)^n] \quad (1)$$

where $F(D)$ —the cumulative percentage of residual under the sieve (%);

R —the cumulative percentage of residual on the sieve (%);

n —the uniformity coefficient, the smaller the n value, the wider the distribution range of material particle size; the larger n is, the narrower the particle size distribution range is.

D_e —characteristic particle size, indicating the homogeneity of the particle group (mm).

The distribution of RRSB is influenced by two parameters, the characteristic particle size D_e and the uniformity coefficient n . The raw ore particle size distribution is adjusted to match a characteristic particle size of $D_e = 0.7$ mm and a corresponding uniformity coefficient of $n = 0.95$. In this experiment, while keeping the characteristic particle size constant, the mass of materials required for each particle size range was calculated by varying the n value. After thorough mixing, jigging was performed as depicted in Figure 3 to investigate the impact of ingredient distribution according to RRSB on jigging separation.

2.3.2. Samples under Fuller Distribution

The Fuller curve distribution is also a two-parameter controlled distribution whose particle size distribution is expressed as follows:

$$U(D_p) = 100 \left(\frac{D_p}{D_{p\max}} \right)^q \quad (2)$$

where U_{D_p} —cumulative percentage under the sieve (%);

$D_{p\max}$ —maximum particle size of the material (mm);

q —distribution modulus, indicating the void ratio between particles, the larger the q , the larger the void ratio; the smaller the q , the smaller the voidage.

According to the feed particle size conditions, the maximum particle size of the material is determined to be $D_{p\max} = 2$ mm. The raw ore particle size distribution is fitted to the corresponding distribution modulus $q = 0.69$, and the maximum particle size of $D_{p\max}$ remains unchanged in this experiment. By varying the q value, the mass of material required for each particle size range is calculated. After mixing for jigging separation, the

material mass is evenly mixed as shown in Figure 4. The effect of ingredient distribution on jigging separation was investigated according to Fuller.

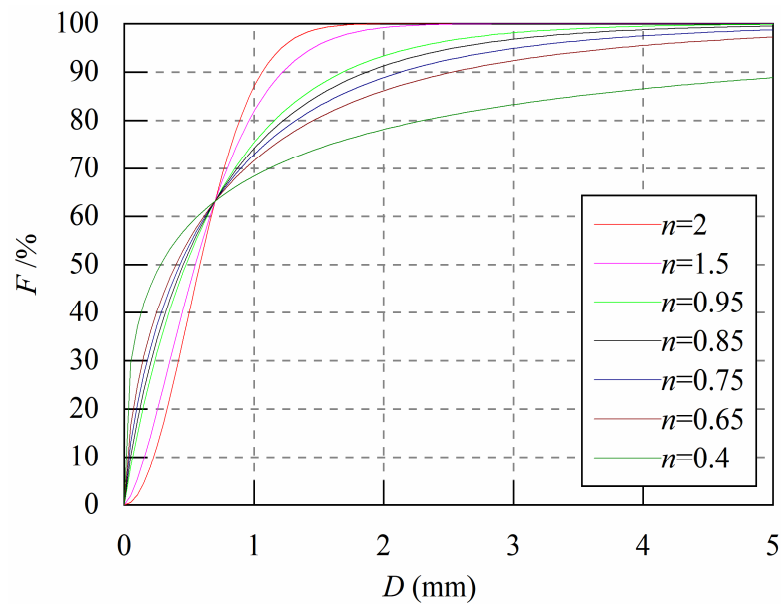


Figure 3. RRSB distribution curve.

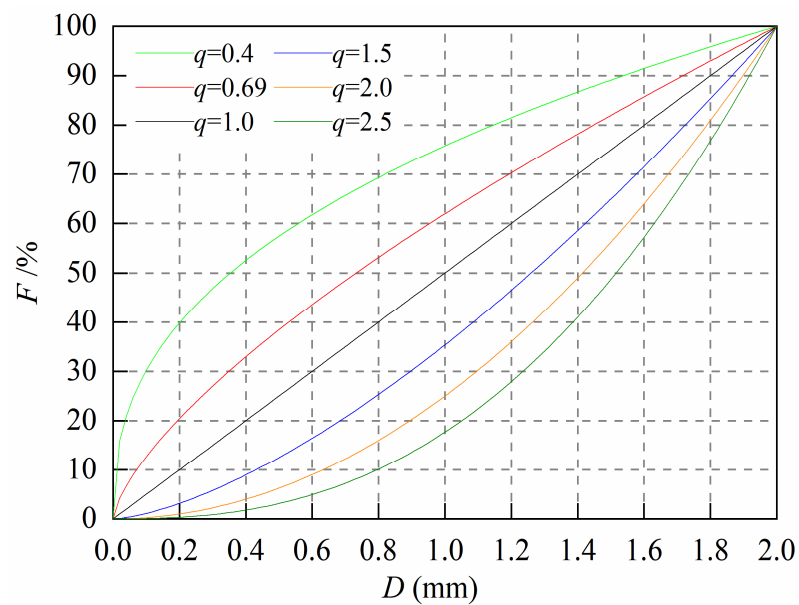


Figure 4. Fuller distribution curve.

2.4. Experimental and Characterization Methods

2.4.1. Experimental Methods

The jig used in the experiment was an XCT diaphragm jig, as shown in Figure 5. The crushed coal gangue particles form a “bed” in the jig machine, which causes periodic vertical alternating water flow in the jig box due to the forced vibration of the transmission mechanism. Under the action of rising water flow, the bed is loose, and the coal gangue particles are gradually stratified according to the particle size, density and shape. At the stage of descending water flow, the bed gradually tightens, and the particles continue to move and layer until most of the particles settle into the sieve plate and stop moving. At this time, only very fine heavy particles can penetrate the cracks of the bed with the descending water flow and drill into the bottom layer. By jigging, the coarse particles

with high density are in the lower layer, the fine particles with high density and the coarse particles with low density are in the middle layer, and the fine particles with low density are in the upper layer, that is, the three products of concentrate, intermediate and tailings. The specific experimental process is shown in Figure 6.



Figure 5. XCT diaphragm jig.



Figure 6. Experimental flow chart.

2.4.2. Characterization Methods

Suitable samples are subjected to heating and drying at a temperature range of 105 °C to 110 °C, followed by grinding to ensure passage through an 80 µm diameter sieve. Subsequently, the samples undergo further heating and drying for a minimum duration of 2 h at a temperature between 105 °C and 110 °C before being removed and stored in a sealed dryer. According to GB/T 27974-2011 “Chemical Analysis Method for fly Ash and Coal Gangue for Building Materials”, the sulfur (S) in the three samples was analyzed using the Eska method (reference method), and the iron (Fe) in them was analyzed using the EDTA direct titration method [37]. The recovery rate of S and Fe in concentrate products and the difference of S and Fe contents in fine tailings were used as the index to evaluate the separation effect.

3. Results

3.1. Distribution Characteristics of Minerals

The mineral distribution granularity of coal gangue is fine, quartz and kaolinite are the main minerals, with quartz being irregularly granularly distributed. Kaolinite is generally loose block; there are also small amounts of calcite and dolomite in coal gangue, calcite is distributed in the form of fragments, and dolomite is mostly distributed in the shape of strips in quartz. Pyrite in coal gangue mainly exists in the form of agglomerated aggregates, with a small and uneven distribution content, as shown in Figure 7a. The average size of pyrite particles in the aggregate is 20 to 30, the average size of aggregate is 6 μm , and the average size of pyrite particles is 1 μm , as shown in Figure 7b.

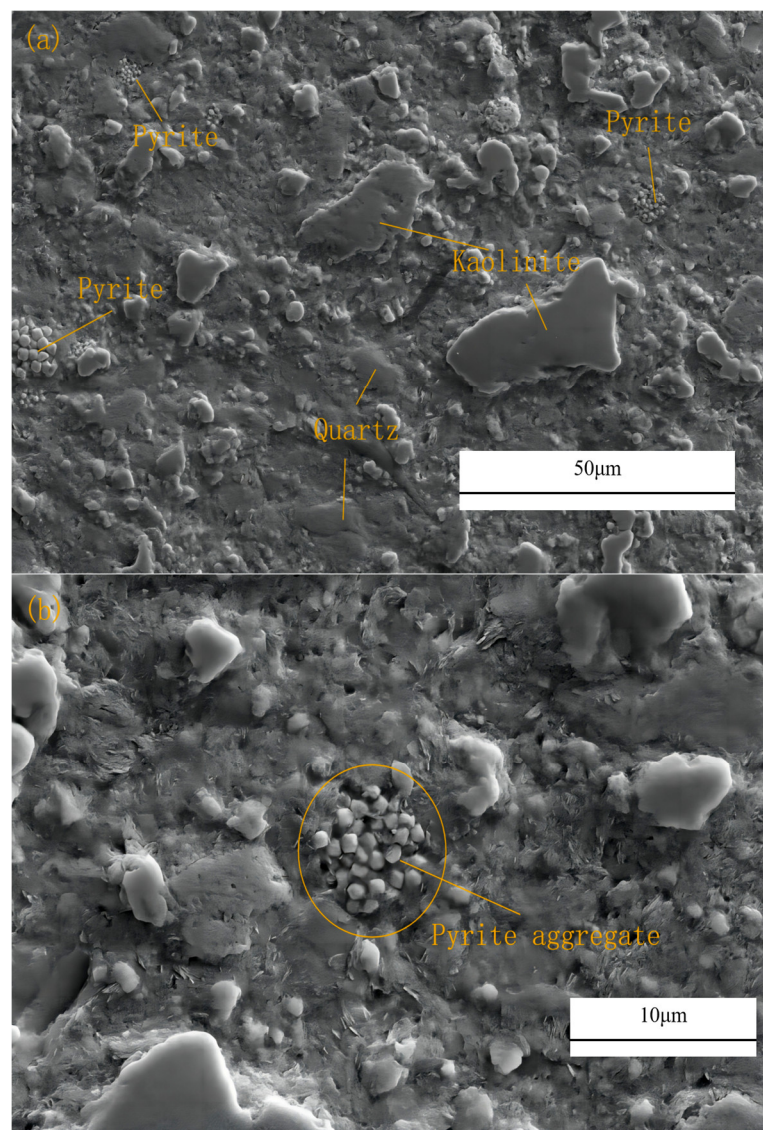


Figure 7. SEM image of coal gangue minerals. (a) Major mineral; (b) Pyrite.

3.2. The Fitting Judgment of the Original Distribution

The grain size distribution of coal gangue was fitted with normal, lognormal, RRSB, and Fuller distributions, as well as the corresponding deterministic coefficients (R^2) of 0.89567, 0.97157, 0.97297, and 0.93954, respectively, as shown in Figure 8. The lognormal distribution is commonly employed in theoretical analysis; however, it exhibits significant linear deviation when applied to particles with a wide range of sizes such as fine powder

materials. In contrast, the RRSB and Fuller distributions provide more accurate descriptions for the original particle size distribution.

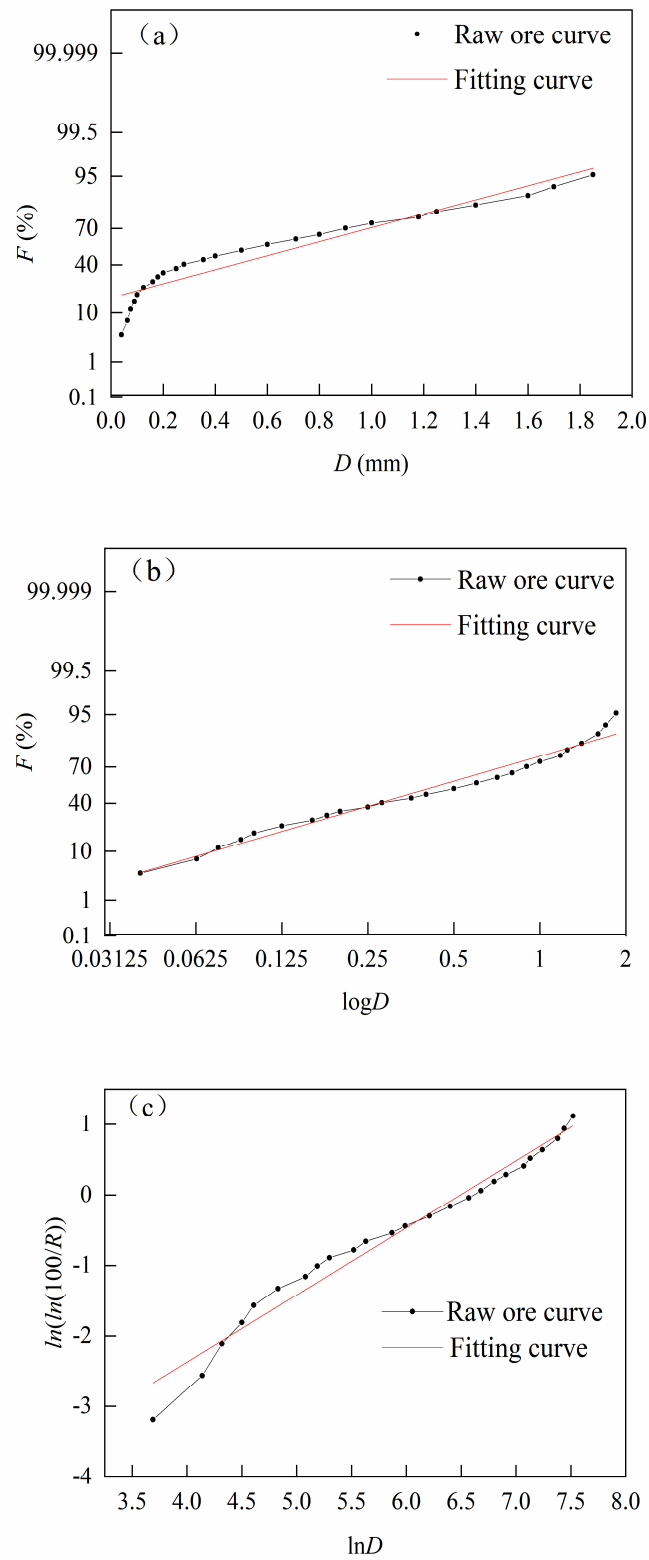


Figure 8. Cont.

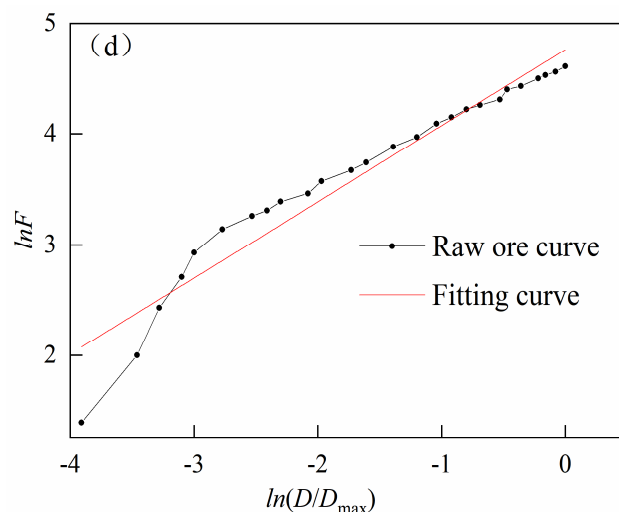


Figure 8. Determination of particle size distribution. (a) Normal fitting; (b) Lognormal fitting; (c) RRSB fitting; (d) Fuller fitting.

3.3. Bed Thickness

The jig bed comprises an artificial bed and a material bed, with the thickness of the jig bed impacting separation efficiency by influencing material looseness and layering speed. Feldspar was chosen as the artificial bed because its density ($2.55\text{--}2.75\text{ g/cm}^3$) was similar to gangue mineral density in the coal gangue and lower than that of concentrate. Moreover, the irregularly shaped feldspar bed prevents the coal gangue from entering the concentrate directly. It not only ensures the tailings discharge rate of jig, but also improves the quality of concentrate. Jigging separation tests were carried out using 10 kg of raw coal gangue crushed to -4 mm under varying bed thickness conditions (5, 6, 7, and 8 cm). The test results are detailed in Table 3.

Table 3. Test results of bed thickness.

Bed Thickness (cm)	Product	Productivity (%)	Content (%)		Concentrate Recovery Rate (%)		Fine Tail Difference (%)	
			S	Fe	S	Fe	S	Fe
5	Concentrate	24.02	4.44	9.63	48.70	43.16	3.22	6.08
	Intermediate	16.47	2.43	5.68				
	Tailings	59.51	1.22	3.55				
6	Concentrate	22.96	4.90	10.20	51.37	43.69	3.77	6.75
	Intermediate	15.84	2.36	5.73				
	Tailings	61.20	1.13	3.45				
7	Concentrate	20.43	5.56	11.92	51.87	45.43	4.58	9.02
	Intermediate	15.22	2.78	6.96				
	Tailings	64.35	0.98	2.90				
8	Concentrate	18.62	5.68	12.11	48.29	42.07	4.48	8.68
	Intermediate	14.68	2.28	5.56				
	Tailings	66.70	1.20	3.43				

With the increase in bed thickness, there is a decrease in the productivity of concentrate and middle ore, an increase in the content of S and Fe, and an increase in the productivity of tailings. The recovery rate of S and Fe, as well as the difference in their contents in the concentrate, initially increases and then decreases with the increase in bed thickness, as shown in Figure 9.

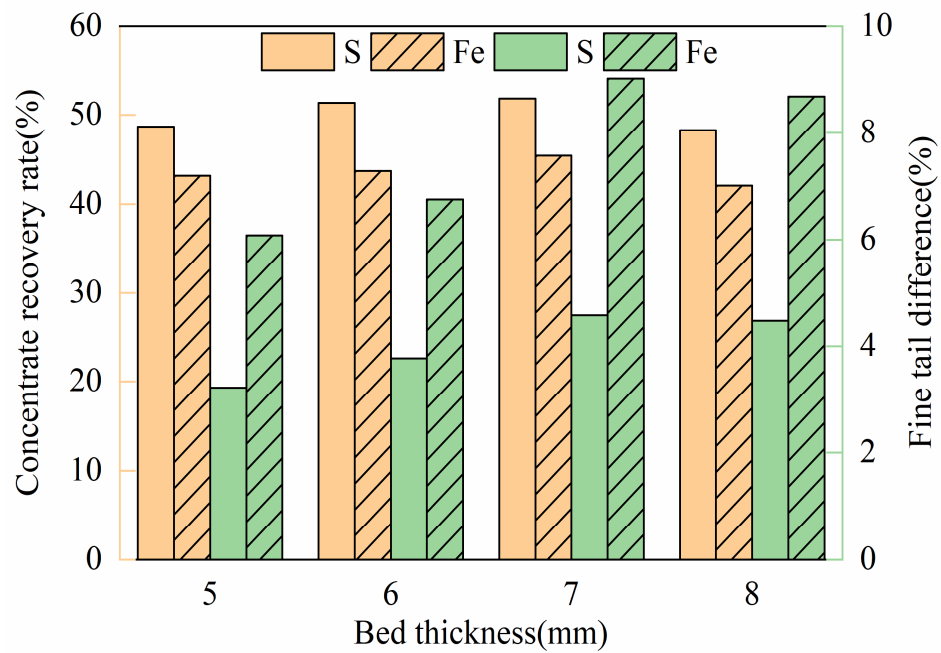


Figure 9. Influence of bed thickness on jigging separation.

3.4. Feed Particle Size

The pyrite in coal gangue is primarily found in the form of agglomerated aggregates, with some existing as monomer particles. Additionally, both types of pyrite in the coal gangue have relatively fine grain sizes, and most of the broken particles still consist of gangue minerals and pyrite. In order to study the influence of particle dissociation degree on jigging separation, the coal gangue was crushed to less than 1, 2, 3 and 4 mm, respectively, under the condition that the bed thickness was 7 cm and other parameters remained unchanged. The test results are shown in Table 4.

Table 4. Test results of feed particle size.

Feed Particle Size (mm)	Product	Productivity (%)	Content (%)		Concentrate Recovery Rate (%)		Fine Tail Difference (%)	
			S	Fe	S	Fe	S	Fe
1	Concentrate	26.83	3.87	8.78	47.41	43.95	2.53	5.21
	Intermediate	8.78	3.32	8.06				
	Tailings	64.39	1.34	3.57				
2	Concentrate	16.51	7.33	15.38	55.26	47.37	6.59	13.05
	Intermediate	16.47	2.93	7.64				
	Tailings	67.02	0.74	2.33				
3	Concentrate	18.40	6.18	13.47	51.92	46.24	5.26	10.81
	Intermediate	15.90	2.80	7.13				
	Tailings	65.70	0.92	2.66				
4	Concentrate	20.43	5.56	11.92	51.87	45.43	4.58	9.02
	Intermediate	15.22	2.78	6.96				
	Tailings	64.35	0.98	2.90				

With the increase in particle size, the productivity of concentrate initially decreases and then increases, while the productivity of tailings initially increases and then decreases. The content of S and Fe in the concentrate first increases and then decreases, whereas in the tailings it first decreases and then increases. The recovery rate of S and Fe, as well as the difference in fineness and tail content of the concentrate, also initially increase before decreasing, as shown in Figure 10.

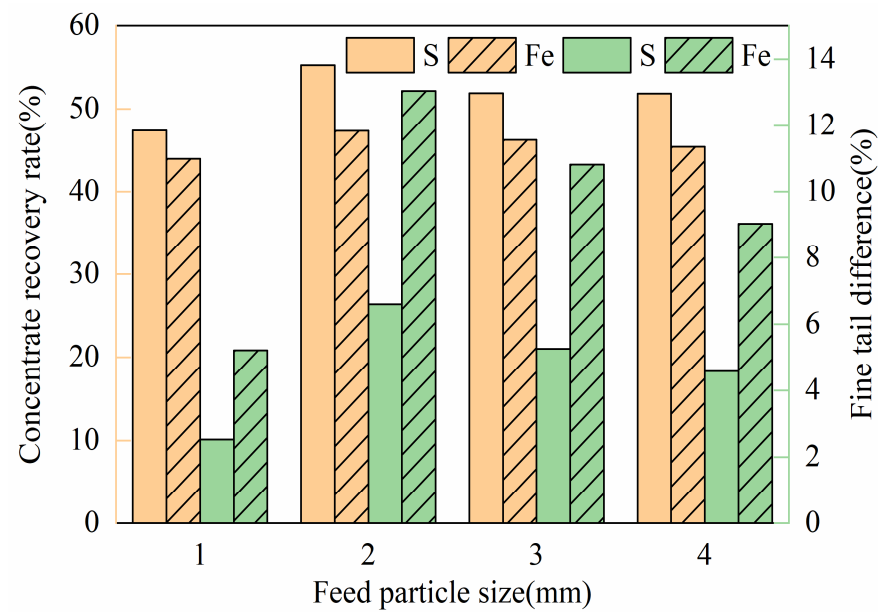


Figure 10. Influence of feed particle size on jigging separation.

3.5. RRSB Distribution

In practical terms, the particle size distribution of coal gangue is continuous, serving as the foundation for RRSB distribution in describing the fine grain grade materials of coal gangue. The calculation was conducted under the RRSB distribution with a characteristic particle size $D_e = 0.70$ mm, based on the distribution curves of seven different uniformity coefficients n values. Materials from various particle size ranges were selected, evenly mixed, and then jig separated. The test results are presented in Table 5.

Table 5. Test results of RRSB distribution.

Coefficient of Uniformity (n)	Product	Productivity (%)	Content (%)		Concentrate Recovery Rate (%)		Fine Tail Difference (%)	
			S	Fe	S	Fe	S	Fe
2.00	Concentrate	16.89	4.94	10.33	38.10	32.55	3.55	6.47
	Intermediate	13.72	2.87	6.85				
	Tailings	69.39	1.39	3.86				
1.50	Concentrate	16.33	5.69	11.02	42.43	33.57	4.44	7.26
	Intermediate	12.84	2.93	6.97				
	Tailings	70.83	1.25	3.76				
0.95	Concentrate	15.68	6.52	13.13	46.68	38.41	5.41	9.77
	Intermediate	12.36	2.98	7.12				
	Tailings	71.96	1.11	3.36				
0.85	Concentrate	15.38	7.68	15.96	53.94	45.80	6.81	13.22
	Intermediate	11.97	3.13	7.66				
	Tailings	72.65	0.87	2.74				
0.75	Concentrate	14.86	7.12	15.24	48.31	42.25	6.12	12.22
	Intermediate	12.43	3.25	7.25				
	Tailings	72.71	1.00	3.02				
0.65	Concentrate	14.40	6.71	14.17	44.12	38.07	5.50	10.73
	Intermediate	12.85	2.70	6.33				
	Tailings	72.75	1.21	3.44				
0.40	Concentrate	13.37	6.32	12.75	38.58	31.80	4.98	8.96
	Intermediate	12.28	2.84	6.80				
	Tailings	74.35	1.34	3.79				

The uniformity coefficient n decreases, the fine mineral productivity decreases continuously, and the contents of S and Fe first increase and then decrease. The tail mineral rate increased continuously, and the contents of S and Fe first decreased and then increased. With the decrease in the n value, the recovery rate of the concentrate and the difference of precision and tail first increased and then decreased, and the inflection point appeared under the RRSB distribution of $n = 0.85$, as shown in Figure 11. When the n value is reduced to 0.85, the best separation effect is obtained, the difference between S and Fe content is 6.81% and 13.22%, and the tail mineral rate also achieves the effect of “tail throwing” by the jig. However, compared with the particle size distribution of raw ore, the separation effect of RRSB distribution based on different n values did not change significantly.

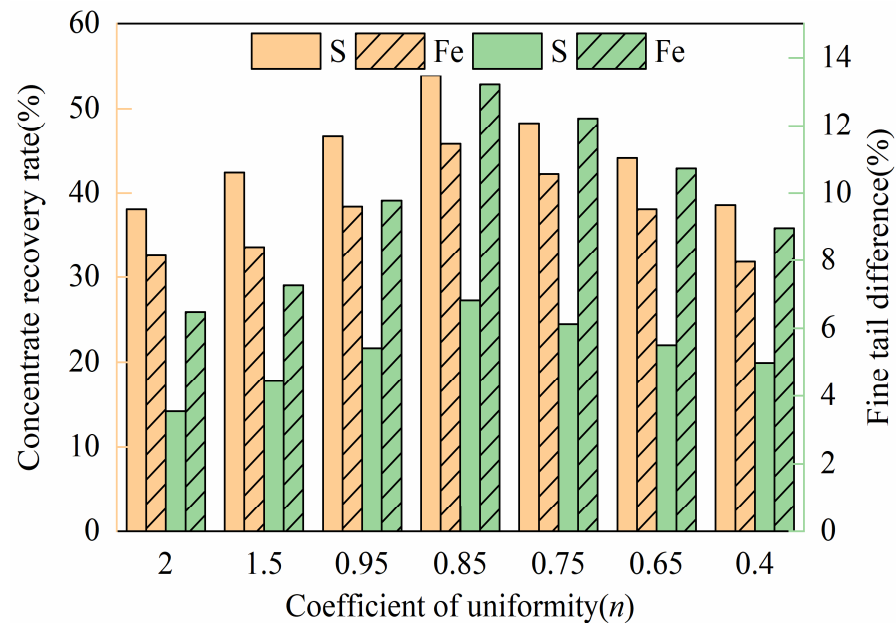


Figure 11. Influence of RRSB distribution on jigging separation.

3.6. Fuller Distribution

The maximum particle size D_{pmax} in Fuller distribution was determined to be 2 mm from the feeding maximum particle size experiment. Based on the distribution curve of six different distribution modulus q values, the calculation was made, materials of various particle size ranges were selected for mixing, and jigging separation was carried out after uniform mixing. The test results are shown in Table 6.

Table 6. Test results of Fuller distribution.

Modulus of Distribution (q)	Product	Productivity (%)	Content (%)		Concentrate Recovery Rate (%)		Fine Tail Difference (%)	
			S	Fe	S	Fe	S	Fe
0.40	Concentrate	14.19	6.38	12.56				
	Intermediate	12.26	2.96	7.46	41.34	33.25	5.13	8.94
	Tailings	73.55	1.25	3.62				
0.69	Concentrate	13.85	6.97	13.84				
	Intermediate	11.34	3.17	7.99	44.08	35.76	5.81	10.45
	Tailings	74.81	1.16	3.39				
1.00	Concentrate	12.84	8.67	16.43				
	Intermediate	10.69	4.13	8.96	50.83	39.36	7.84	13.43
	Tailings	76.47	0.83	3.00				

Table 6. Cont.

Modulus of Distribution (q)	Product	Productivity (%)	Content (%)		Concentrate Recovery Rate (%)		Fine Tail Difference (%)	
			S	Fe	S	Fe	S	Fe
1.50	Concentrate	12.06	9.59	18.26	52.81	41.09	8.88	15.54
	Intermediate	9.69	4.96	10.62				
	Tailings	78.25	0.71	2.72				
2.00	Concentrate	11.67	8.50	17.13	45.29	37.30	7.45	13.94
	Intermediate	10.23	3.69	8.51				
	Tailings	78.1	1.05	3.19				
2.50	Concentrate	11.20	7.33	15.62	37.49	32.64	6.03	12.10
	Intermediate	11.11	3.23	7.86				
	Tailings	77.69	1.30	3.52				

With the increase of distribution modulus q , the productivity of concentrate decreased, and the contents of S and Fe first increased and then decreased. The contents of S and Fe in tailings first decreased and then increased. With the decrease in the q value, the recovery rate of concentrate and the fine tail difference first increased and then decreased, as shown in Figure 12.

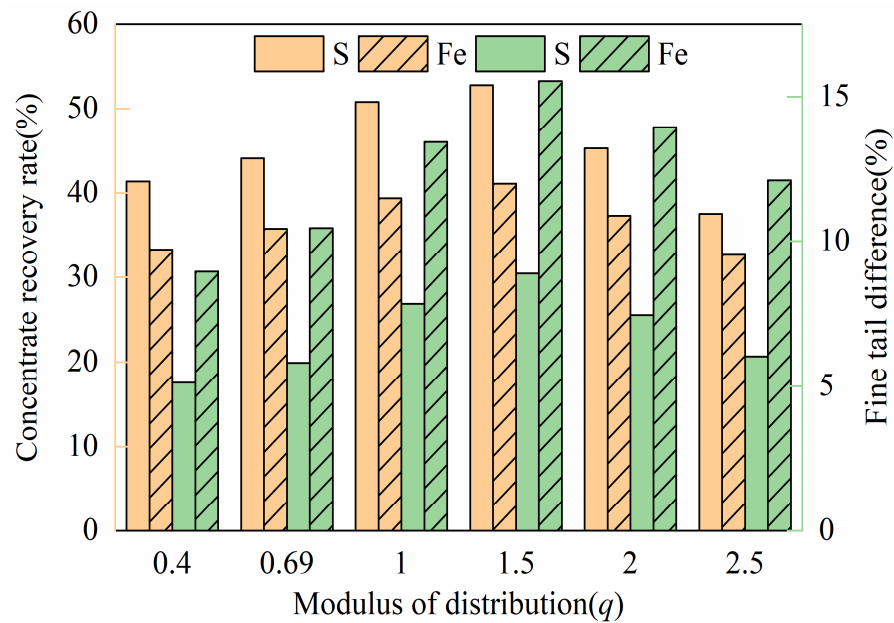


Figure 12. Influence of Fuller distribution on jigging separation.

4. Discussion

The material entering the jig is stacked on the sieve and strictly stratified along the bed thickness according to density. The stress experienced by ore particles during the jigging process is a complex phenomenon. Without considering the interaction between particles, it is generally believed that the ore particles in the jigging process are subjected to the comprehensive action of three forces: water flow force, gravity and drag force [38]. In the process of the jig separation of coal gangue ore particles, the flow force acts on the cross-section of the particles, the gravity of the ore particles is vertical downward, and the drag force is the force opposite to the direction of the movement of the ore particles [39,40]. Under the comprehensive action of the three forces, coal gangue grains undergo reciprocating lifting and settling movements. The characteristic coefficients of mineral particles' movement characteristics, such as force, acceleration, and velocity in the separation process, vary due to differences in mineral density and particle size within the material. Different

ore particles with varying movement characteristics are utilized to achieve appropriate bed looseness during jiggling. A thicker bed results in a higher accumulation height on the sieve, while a more complete motion process under combined force facilitates the formation of a bed with suitable looseness and optimal layering speed. However, changes in bed thickness have little impact on jiggling separation compared to raw ore S and Fe content. After comprehensive consideration of separation index, 7 cm was determined as the best bed thickness.

In the coal gangue raw ore broken and dissociated by a jaw crusher, the proportion of pyrite monomer minerals is relatively small, with most still existing as connected ore objects. A smaller feed particle size results in a larger proportion of broken and dissociated monomer minerals, leading to an improved separation effect. The jiggling separation effect of -1 mm material is inferior compared to the other three groups. When the particle size is too small, it leads to a “layer collapse” effect, making it difficult for fine particles to form an appropriate bed looseness with the artificial bed. As a result, they either directly enter the tailings under the transverse flow force or penetrate into the concentrate through drilling. This leads to a decrease in middle ore productivity, an increase in concentrate productivity, and a decrease in S and Fe content as well as recovery rate. The optimal separation effect is achieved when the feeding particle size is -2 mm according to the comprehensive separation index. At this point, we can obtain concentrate with a productivity of 16.51%, S and Fe contents of 7.33% and 15.38%, and tailings with a productivity of 67.02%, as well as a S and Fe contents of 0.74% and 2.33%. Furthermore, based on separation results, it is evident that particle size has a significant impact on coal gangue separation; therefore, determining particle size is crucial for pre-crushing and sieving on jiggling separation. Mahmoud M. Ahmed also separated coal gangue from two factors of bed thickness and feed particle size. Under the condition of a feed particle size of 3.907 mm and a bed thickness of 1.87 cm, concentrate product with a recovery rate of 97.74% was obtained [41]. This is sufficient in proving that the separation effect can be effectively improved by changing the bed thickness and feed particle size.

For RRSB distribution, under the condition of constant characteristic particle size, the smaller the n value, the wider the particle size distribution range of the material, and the more particles with different particle size and density in the material. There are also differences in the motion states of the particle groups during jig settling and lifting. In the lifting process of the water flow, the particles with small particle size move faster, while the particles with large particle size move slower. In the sedimentation process of water flow, the particles with large particle size move fast, and the particles with small particle size move slowly. Whether in the process of lifting or settling, there is often a phenomenon of “equal settling”, that is, some of the ore particles with large particle size and low density move at the same speed as the ore particles with small particle size and high density. The motion characteristics of the material particles located above and below the isosetting particle group are different. This is also the reason why the material is stratified according to density and particle size in the jiggling separation process. From the perspective of the separation effect, the separation effect is gradually improved when the n value drops from 2 to 0.85. When n value decreases from 0.85 to 0.4, the separation effect gradually decreases. This indicates that when $n = 0.85$, not only is the loose degree of accumulated material bed suitable, but the degree of material dissociation of graded ingredients according to RRSB distribution is also better.

For Fuller distribution, when $q = 1.0$, 0~1 mm material and 1~2 mm material account for 50% each, and the mass proportion of 0~1 mm material is smaller than that of raw ore particle size distribution, while the mass proportion of 1~2 mm material is larger than that of raw ore particle size distribution. At this time, the separation effect is significantly improved compared with the particle size distribution of the raw ore, and it is also better than the separation effect under the $n = 0.85$ RRSB distribution, which further verifies that the particle size composition of the material has an effect on the jiggling separation. With the increase of the q value to 1.5, the separation effect is further improved and reaches the

peak, and the concentrates and tailings with a difference of S and Fe content of 8.88% and 15.54% can be obtained by separation. Compared with the separation effect under the size distribution of raw ore, the contents of S and Fe in concentrates are increased by 2.26% and 2.88%, while the contents of S and Fe in tailings are reduced by 0.21% and 0.14%.

For a Fuller distribution with a maximum particle size D_{pmax} of 2 mm, the proportion of coarse particles in the material increases with an increase in the q value. Compared to the distributions of fine-grained materials with a larger proportion, distributions of coarse-grained materials containing feldspar are more conducive to forming beds with suitable looseness. The composition of materials with different particle sizes affects the looseness of the bed formed by the particle group and the artificial feldspar bed. From a separation perspective, a higher q value does not necessarily result in better outcomes; rather, at a certain q value, achieving optimal separation effects requires appropriate levels of bed looseness and particle dissociation. The best separation effect under RRSB distribution is close to that under Fuller distribution, while the best separation effect under Fuller distribution is further improved compared with the separation effect under other parameters [42,43] (bed thickness, feed size, stroke and water volume, etc.).

The principle governing the impact of Fuller distribution and RRSB distribution on jigging separation is consistent, as the particles' varying size and density affect the bed porosity and layering speed of stacked materials. The distinction lies in the fact that for RRSB distribution, the separation effect initially increases and then decreases with a decrease in the uniformity coefficient n . In contrast, for Fuller distribution, the separation effect first increases and then decreases with an increase in distribution modulus q . When comparing the separation effects under these two distributions, it can be concluded that based on Fuller distribution, the separation effect is superior to that of RRSB distribution.

5. Conclusions

In this experiment, the ore properties of coal gangue are tested and analyzed. Subsequently, the coal gangue is crushed to -2 mm, sieved, and a grain size distribution curve is plotted. The bed thickness and feed particle size of coal gangue with raw particle size distribution were tested. Then, the fitting of the raw particle size distribution is determined, followed by jigging separation based on RRSB distribution and Fuller distribution.

The bed thickness and feed particle size conditions were tested for the raw particle size distribution of coal gangue, and the best separation effect was obtained under the optimal parameters of bed thickness 7 cm and feed size 2 mm, with a S, Fe content difference of 6.59% and 13.05% in the concentrate and tailings.

The particle size distribution of coal gangue raw ore was determined to be more consistent with the RRSB distribution and Fuller distribution after fitting. The separation effect based on the RRSB distribution feeding material with a uniformity coefficient n decreased first and then increased as the value decreased. The separation effect of coal gangue based on the RRSB distribution with a uniformity coefficient $n = 0.85$ was the best, with a S, Fe content difference of 6.81% and 13.22% in the concentrate and tailings, but the improvement in separation effect compared to the original particle size distribution was not significant.

Additionally, the separation effect based on the Fuller distribution feeding material with a distribution modulus q increased first and then decreased as the value increased. The separation effect of coal gangue based on the Fuller distribution with a distribution modulus $q = 1.50$ was the best, with a S, Fe content difference of 8.88% and 15.54% in the concentrate and tailings; compared to the raw ore, the S, Fe content in the concentrate increased by 5.49% and 10.60%; compared to the $n = 0.85$ RRSB distribution, the S, Fe content in the concentrate increased by 1.91% and 2.30%, and the separation effect was significantly improved.

The principle of influencing the separation effect of the RRSB distribution and Fuller distribution in the material feeding for the jigging separation is the same, which is to influence the looseness and layering speed of the bed material formed by the different

particle size and density of the material composition, thereby affecting the separation effect. The tailings produced under the two distributions have low S and Fe content and can be directly used as raw materials for building materials. Compared with the separation effect under the optimal parameters, for the fine-grained gangue, the material feeding based on the Fuller distribution for the jigging separation is better than that based on the RRSB distribution.

Author Contributions: Conceptualization—X.H. and Z.X.; Methodology—X.H. and Z.X.; Validation—Z.X.; Investigation—Z.X.; Writing—original draft preparation—Z.X.; Writing—review and editing—X.H.; Supervision—X.W. and W.J.; Project administration—X.H. and Z.X.; Funding acquisition—X.H. All authors have read and agreed to the published version of the manuscript.

Funding: This work was funded by the Key Research and Development Plan of Shaanxi Province, and the funding number is 2024GX-YBXM-572.

Institutional Review Board Statement: Not applicable.

Informed Consent Statement: Not applicable.

Data Availability Statement: The raw and processed data required to reproduce these results are available upon reasonable request.

Conflicts of Interest: The author declares no conflicts of interest.

References

- Du, T.; Wang, D.M.; Bai, Y.J.; Zhang, Z.Z. Optimizing the formulation of coal gangue planting substrate using wastes: The sustainability of coal mine ecological restoration. *Ecol. Eng.* **2020**, *143*, 105669. [[CrossRef](#)]
- Lu, S.H.; Pan, J.; Zhu, D.Q.; Guo, Z.Q.; Li, S.W.; Shi, Y.; Zhang, W.J. Investigation on activation technology of self-heating decarbonization of coal gangue by a sintering process. *J. Cent. South Univ.* **2023**, *30*, 1158–1167. [[CrossRef](#)]
- Zhang, H.L.; Shu, Y.X.; Yue, S.L.; Chen, Y.Q.; Mikulcic, H.; Rahman, Z.U.; Tan, H.Z.; Wang, X.B. Preheating pyrolysis-char combustion characteristics and kinetic analysis of ultra-low calorific value coal gangue: Thermogravimetric study. *Appl. Therm. Eng.* **2023**, *229*, 120583. [[CrossRef](#)]
- Jiang, X.Y.; Zhao, C.; Hu, X.M.; Tong, Z.F.; Yun, J.G.; Wei, N.H.; Wang, K.J.; Liu, C.X.; Zou, Y.; Chen, Z.H. Utilization of coal gangue for preparing high-silica porous materials with excellent ad/desorption performance on VOCs. *J. Chem. Technol. Biotechnol.* **2022**, *97*, 3498–3510. [[CrossRef](#)]
- Liu, L.H.; Liu, Q.F.; Zhang, K.A.; Zhang, S.; Li, K.; Li, J.T.; Peng, G.Y. Correction: Thermal decomposition and oxidation of pyrite with different morphologies in the coal gangue of North China. *J. Therm. Anal. Calorim.* **2023**, *148*, 2039–2040. [[CrossRef](#)]
- Li, X.Y.; Qiao, Y.J.; Shao, J.H.; Bai, C.Y.; Li, H.Q.; Lu, S.; Zhang, X.H.; Yang, K.; Colombo, P. Sodium-based alkali-activated foams from self-ignition coal gangue by facile microwave foaming route. *Ceram. Int.* **2022**, *48*, 33914–33925. [[CrossRef](#)]
- Chen, Z.H.; Huang, X.Y.; He, H.; Tang, J.L.; Tao, X.X.; Huang, H.Z.; Haider, R.; Ali, M.I.; Jamal, A.; Huang, Z.X. Bioleaching Coal Gangue with a Mixed Culture of *Acidithiobacillus ferrooxidans* and *Acidithiobacillus thiooxidans*. *Minerals* **2021**, *11*, 1043. [[CrossRef](#)]
- Ren, B.K.; Chai, L.J.; Liu, Y.Z.; Wang, Y.K. Preparation of High-Ductility Cement-Calcined Coal-Gangue-Powder-Composite-Based Rapid Repair Material. *Materials* **2023**, *16*, 6049. [[CrossRef](#)] [[PubMed](#)]
- Jiang, J.H.; Han, Y.F.; Zhao, H.J.; Suo, J.L.; Cao, Q.B. Recognition and sorting of coal and gangue based on image process and multilayer perceptron. *Int. J. Coal Prep. Util.* **2023**, *43*, 54–72. [[CrossRef](#)]
- Hacifazlioglu, H. A new process for the production of medium quality fuels from coal washing plant coarse tailings. *Energy Sources Part A-Recovery Util. Environ. Eff.* **2016**, *38*, 2809–2815. [[CrossRef](#)]
- Oparin, V.N.; Ordin, A.A. Hubbert's Theory and the Ultimate Coal Production in Temrs of the Kuznetsk Coal Basin. *J. Min. Sci.* **2011**, *47*, 254–266. [[CrossRef](#)]
- Phengsaart, T.; Park, I.; Pasithbhattarabhorn, J.; Srichonphaisarn, P.; Kertbundit, C.; Phumkokrux, N.; Juntarasakul, O.; Tabelin, C.B.; Hiroyoshi, N.; Ito, M. Development of Microencapsulation-Hybrid Jig Separation Technique as a Clean Coal Technology. *Energies* **2023**, *16*, 2432. [[CrossRef](#)]
- Viduka, S.; Feng, Y.Q.; Hapgood, K.; Schwarz, P. CFD-DEM investigation of particle separations using a sinusoidal jigging profile. *Adv. Powder Technol.* **2013**, *24*, 473–481. [[CrossRef](#)]
- Andavarapu, M.R.; Vidyadhar, A.; Prasad, R.; Sahoo, M. Efficacy of Pilot Scale Batac Jig on LVC Coal Utilization for Coke Making. *Trans. Indian Inst. Met.* **2023**, *76*, 1553–1561. [[CrossRef](#)]
- Surowiak, A. The analysis of coal fines separation precision exposed to changeable hydrodynamic parameters of jig work. *Arch. Min. Sci.* **2018**, *63*, 437–448. [[CrossRef](#)]
- Cierpisz, S. On-line monitoring of a coal separation process in a jig—A simulation study. *Gospod. Surowcami Miner.* **2018**, *34*, 41–52. [[CrossRef](#)]

17. Niedoba, T.; Surowiak, A.; Hassanzadeh, A.; Khoshdast, H. Evaluation of the Effects of Coal Jigging by Means of Kruskal-Wallis and Friedman Tests. *Energies* **2023**, *16*, 1600. [[CrossRef](#)]
18. Mort, P. Analysis and graphical representation of particle size distributions. *Powder Technol.* **2023**, *420*, 118100. [[CrossRef](#)]
19. Luo, Q.S.; Wang, S.; Guo, Y.C.; He, L.; Li, X. Adaptive image enhancement and particle size identification method based on coal and gangue. *Meas. Sci. Technol.* **2023**, *34*, 105403. [[CrossRef](#)]
20. Zeller, C.B.; Cabral, C.R.B.; Lachos, V.H.; Benites, L. Finite mixture of regression models for censored data based on scale mixtures of normal distributions. *Adv. Data Anal. Classif.* **2019**, *13*, 89–116. [[CrossRef](#)]
21. Foster, C.R. Estimating the Lognormal Size Distribution of Spheres by Plane Sampling. *Metall. Mater. Trans. A-Phys. Metall. Mater. Sci.* **2022**, *53*, 3507–3511. [[CrossRef](#)]
22. Guan, J.F.; Li, Y.; Bai, W.F.; Hao, Y.; Yin, Y.A.; Yang, B.A. A simple fracture model for dam concrete based on the Fuller and Thompson formula. *Fatigue Fract. Eng. Mater. Struct.* **2022**, *45*, 3210–3236. [[CrossRef](#)]
23. Lv, H.G.; Zhang, X.Y.; Huang, G.; Li, J.H.; Ma, L.Q. Online analysis of coal slime water particle size based on RRSB characteristic parameters. *Int. J. Coal Prep. Util.* **2022**, *42*, 3185–3201. [[CrossRef](#)]
24. Cui, Y.P.; Liu, J.; Wang, L.C.; Liu, R.Q.; Pang, B. Effect of Fly Ash with Different Particle Size Distributions on the Properties and Microstructure of Concrete. *J. Mater. Eng. Perform.* **2020**, *29*, 6631–6639. [[CrossRef](#)]
25. Gao, P.; Zhang, T.S.; Wei, J.X.; Yu, Q.J. Evaluation of RRSB distribution and lognormal distribution for describing the particle size distribution of graded cementitious materials. *Powder Technol.* **2018**, *331*, 137–145. [[CrossRef](#)]
26. Sun, W.C.; Wu, K.; Huang, H.B. A graded granular material generation algorithm based on particle number probability distribution by DEM. *Phys. A* **2021**, *573*, 125919. [[CrossRef](#)]
27. Chen, Z.; Li, B.X.; Zhang, Q.; Hu, X.D.; Ding, Y.; Zhu, Z.X.; Xiao, P.; Liang, S.H. W-Cu Composite with High W Content Prepared by Grading Rounded W Powder with Narrow Particle Size Distribution. *Materials* **2022**, *15*, 1904. [[CrossRef](#)]
28. Qiu, P.Y.; Pabst, T. Characterization of particle size segregation and heterogeneity along the slopes of a waste rock pile using image analysis. *Environ. Earth Sci.* **2023**, *82*, 573. [[CrossRef](#)]
29. Piepho, H.P. An adjusted coefficient of determination (R^2) for generalized linear mixed models in one go. *Biom. J.* **2023**, *65*, e2200290. [[CrossRef](#)]
30. Nakagawa, S.; Johnson, P.C.D.; Schielzeth, H. The coefficient of determination R^2 and intra-class correlation coefficient from generalized linear mixed-effects models revisited and expanded. *J. R. Soc. Interface* **2017**, *14*, 20170213. [[CrossRef](#)]
31. Chaurasia, A.; Harel, O. Partial F -tests with multiply imputed data in the linear regression framework via coefficient of determination. *Stat. Med.* **2015**, *34*, 432–443. [[CrossRef](#)]
32. Dang, W.; He, H.Y. Comprehensively utilizing waste coal gangue to fabricate high strength glass-ceramics. *J. Ceram. Process. Res.* **2020**, *21*, 69–74. [[CrossRef](#)]
33. Zhang, Q.H.; Jia, X.L.; Wang, D. Experimental evaluation of the effect of sulfur content on the spontaneous combustion characteristics parameters of coal. *Thermochim. Acta* **2024**, *732*, 179651. [[CrossRef](#)]
34. Yang, C.G.; Yin, J.Q.; Wu, L.Q.; Zeng, Q.Y.; Zhang, L.W. Research on the Identification Mechanism of Coal Gangue Based on the Differences of Mineral Components. *ACS Omega* **2023**, *8*, 48–55. [[CrossRef](#)]
35. Zhou, C.C.; Liu, G.J.; Yan, Z.C.; Fang, T.; Wang, R.W. Transformation behavior of mineral composition and trace elements during coal gangue combustion. *Fuel* **2012**, *97*, 644–650. [[CrossRef](#)]
36. Paul, S.R.; Bhattacharya, S. Size by Size Separation Characteristics of a Coal Cleaning Jig. *Trans. Indian Inst. Met.* **2018**, *71*, 1439–1444. [[CrossRef](#)]
37. GB/T 27974-2011; Methods for Chemical Analysis of Fly Ash and Coal Gangue for Building Materials. General Administration of Quality Supervision, Inspection and Quarantine of the People's Republic of China. Standardization Administration of China: Beijing, China, 2011; p. 28.
38. Zhang, J.; Tao, Y.J.; Kuang, Y.L.; Gui, X.H.; Wang, Z.G. Research on particle stratification inside the model jig wash box based on high-speed dynamic analyzer. *Energy Sources Part A-Recovery Util. Environ. Eff.* **2020**, *42*, 641–652. [[CrossRef](#)]
39. Viduka, S.M.; Feng, Y.Q.; Hapgood, K.; Schwarz, M.P. Discrete particle simulation of solid separation in a jigging device. *Int. J. Miner. Process.* **2013**, *123*, 108–119. [[CrossRef](#)]
40. Crespo, E.F. Modeling segregation and dispersion in jigging beds in terms of the bed porosity distribution. *Miner. Eng.* **2016**, *85*, 38–48. [[CrossRef](#)]
41. Ahmed, M.M. Optimization of A Jigging Process Using Statistical Technique. *Int. J. Coal Prep. Util.* **2011**, *31*, 112–123. [[CrossRef](#)]
42. Tripathy, A.; Panda, L.; Sahoo, A.K.; Biswal, S.K.; Dwari, R.K.; Sahu, A.K. Statistical optimization study of jigging process on beneficiation of fine size high ash Indian non-coking coal. *Adv. Powder Technol.* **2016**, *27*, 1219–1224. [[CrossRef](#)]
43. Rastialhosseini, S.A.; Abdollahzadeh, A.A. Effect of feed-size segregation on energy consumption during jigging: A CFD-DEM study. *Part. Sci. Technol.* **2024**, *42*, 565–575. [[CrossRef](#)]

Disclaimer/Publisher's Note: The statements, opinions and data contained in all publications are solely those of the individual author(s) and contributor(s) and not of MDPI and/or the editor(s). MDPI and/or the editor(s) disclaim responsibility for any injury to people or property resulting from any ideas, methods, instructions or products referred to in the content.